SASEC
1st Southern African Solar Energy Conference
21-23 May 2012

TARGET ALIGNED HELIOSTAT FIELD LAYOUT FOR NON-FLAT TERRAIN

Dr. Reiner Buck[1], Andreas Pfahl[1], and Thomas H. Roos[2]

[1] Deutsches Zentrum für Luft- und Raumfahrt (DLR), Pfaffenwaldring 38-40, D-70569 Stuttgart, Germany,
Phone: +49 711 6862 602; Fax: +49 711 6862; E-Mail: reiner.buck@dlr.de. / andreas.pfahl@dlr.de

[2] CSIR; E-mail: throos@csir.co.za

Abstract

The layout for a solar tower test facility for CSIR, Pretoria, is described. The solar tower system is designed for 400kWth receiver outlet power. The heliostat field layout takes into account both the real (non-flat) topography of the terrain as well as the typical weather conditions at the site, with usually better solar conditions in morning times. As first step, an initial field layout was done assuming standard heliostats. Then, the performance improvement due to the use of target-aligned heliostats was evaluated, showing nearly 12% gain in annual energy when optimized canting angles are applied to each heliostat.

In a second step the positions of the heliostats were adjusted to further improve the annual energy yield. This was done by slightly shifting the position of a heliostat and evaluating the impact on annual energy yield. No restrictions were made on the heliostat positions, except for a minimum distance between neighbouring heliostats. The heliostats were repositioned one after the other for the whole field. This procedure was repeated many times. At the end of this optimization, the annual intercepted energy was about 5.1% higher than the initial configuration with target-aligned heliostats.

Keywords: solar tower, heliostat field layout, ray tracing, target aligned heliostat, canting angle

1. Introduction

South Africa has regions with solar insolation levels belonging to the highest available on earth. This is one of the reasons why there is currently increasing interest in exploiting solar energy resources for power production. Besides photovoltaics, concentrating solar power (CSP) technologies are considered promising, mainly due to their ability to deliver dispatchable power. The first commercial solar power plants are in preparation now in South Africa..

In this context the Council for Scientific and Industrial Research (CSIR) in Pretoria intends to install a solar tower test facility enabling solar technology development and training of people. The motivation for this facility, its intended applications and a preliminary layout have already been presented [1]. DLR was subcontracted to do the solar field layout for this solar tower test facility. This heliostat field is different from others in two respects.

Firstly, a usual solar tower field layout assumes flat terrain. Then heliostats are placed according to predefined correlations (e. g. radially staggered). There are no correlations known that are specifically adapted to non-flat terrain. However, some codes can take the actual terrain into account, by assigning a different altitude level to each heliostat. The paper describes the layout procedure and results for the terrain foreseen for the CSIR solar tower test facility. This terrain has an altitude difference of nearly 3m in the region where the heliostat field is to be erected. This difference is not created by a constant slope, but is irregular and can thus not be expressed by simple slope correlations.

Secondly, instead of the conventional T-design heliostat configuration, this heliostat field will make use of heliostats of the target-aligned type. It has been shown by different researchers ([2], [3], [4], [5]) that incorporating different radii of curvature in the sagittal and tangential planes in target-aligned heliostats, the

astigmatism effects can be greatly reduced, increasing flux intensity and decreasing focal spot size throughout the day. While no software codes exist to do the layout of target-aligned heliostat fields in an acceptable time, a preliminary layout using T-type field layout design software can be used as a starting point in a target-aligned field optimization.

2. Layout Data and Assumptions

2.1. CSIR Site Information

It was decided to locate the solar facility on the Pretoria campus at CSIR if possible, for several reasons. It would facilitate the physical security of the solar research equipment, it is convenient due to proximity to CSIR researchers and supporting onsite laboratories, it would allow convenience of access for stakeholders and off-site researchers from academia and industry, and finally the solar resource was considered sufficient. A site in an undeveloped area in the North-West corner of the CSIR campus was identified (shown in Figure 1). The site is gently sloping, quasi-circular in shape and of large enough size: DLR preliminary studies showed the site capable of supporting a 4.2MW_{th} field, much larger than the 500 kW_{th} required.

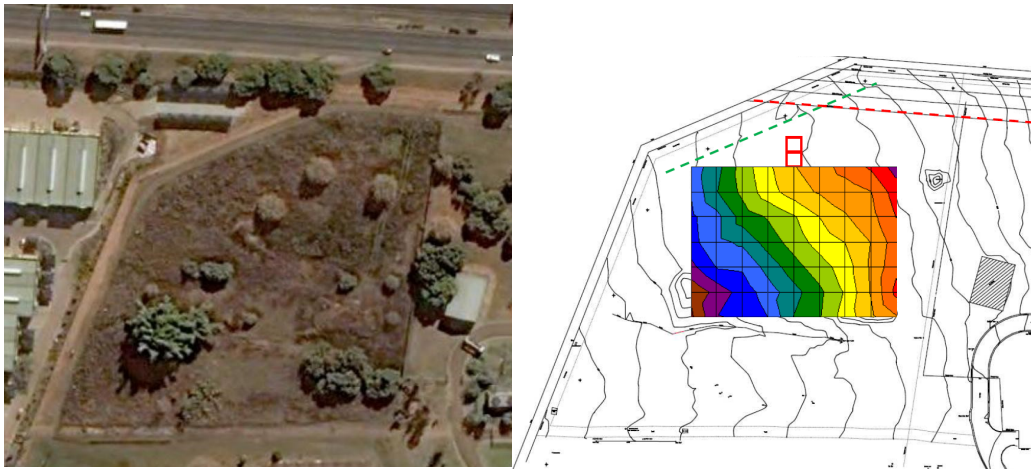

Figure 1: CSIR heliostat field site: Google Earth image (left) and contour map (right), showing 60 m by 80 m area of interest, with 10m grid

The site has some disadvantages, however. A screening wall one heliostat high is required to shield traffic on the highway north of the site, and businesses west of the site boundary (both visible in Figure 1), from heliostat glint. Also, the soil is sandy and not ideal for building. This does not present too much of a problem for heliostats but will require piles for the tower.

2.2 Solar Insolation Assumptions

For the solar system layout September 21 at solar noon was assumed as design point (DP). A DNI of 925W/m² was assumed for design point.

It is customary when designing and analysing renewable energy infrastructure, particularly solar infrastructure, to make use of meteorological data files comprising a typical meteorological year (TMY). This allows performance calculations to be based on statistically probable data, rather than ideal data. Such a dataset was readily available in the form of an International Weather for Energy Calculation (IWEC) Energy Plus Weather (EPW) file, for a location (latitude -26.13°, longitude 28.23°) in Johannesburg.

Pretoria (where CSIR is situated) and Johannesburg are only 50km apart and both cities experience the same weather patterns: dry winters characterised by generally cloudless skies and summers by intermittent cloud cover, often involving days that begin with sunny mornings leading to afternoons with increasing cloud cover, sometimes with thunderstorms. The EPW file data was therefore considered representative of Pretoria, although Johannesburg at 1753m elevation reliably experiences temperatures 2°C cooler than Pretoria at

1366m.

Figure 2 (left) shows the monthly averages of the hourly DNI data from the EPW file, and adds up to a total of 1782kWh/m^2/year, or 4.881kWh/m^2/day. It can be seen that the use of monthly averages leads to low design DNI values, exceeding 800W/m^2 only in July between 12:00 and 14:30, while in February marginally exceeding only 400W/m^2 between 10:00 and 13:00, reaching a maximum of 423W/m^2 at 12:00. On clear sky days in February, however, the maximum values exceed 1000W/m^2 between 11:00 and 14:45! In formations of cumulous clouds, more than other types such as cirrus or stratus, discrete breaks tend to occur, giving rise to a rapid change in DNI experienced on the ground. In significantly cloudy weather incorporating predominantly cumulous clouds (such as in February), if a solar plant operator were to attempt to compensate for the low DNI by using noticeably more heliostats than would be used during clear skies for the same time of day, a break in the clouds would result in concentrated flux at the receiver aperture exceeding the receiver design value, resulting in damage to the receiver before heliostats would have had time to defocus.. For that reason it is not useful to incorporate significantly cloudy data in the design process. A modified hourly design DNI file was then compiled:

- All hourly DNI values below 50W/m^2 were set to 0W/m^2
- In the central portion of the day every hourly DNI value not lying within 25% of the clear-sky value (highest value for the same hour at a different day in the same month) was set to 0W/m^2
- In the early morning and late afternoon of the day every hourly DNI value not lying within 30% of the clear-sky value was set to 0W/m^2.

The rationale behind the filter in bullets 2 and 3 is that the effects of suspended aerosols and cirrus clouds (which are not expected to part) are allowed for, but not cumulous clouds (which run the risk of parting). For each hour of the day, there were an average of 24 non-zero DNI values a month for the four winter months and 7.5 for the four summer months.

For each month of the year, a single representative day was constructed, where for each daylight hour of the day, a value was chosen representing the spread of values allowed through the filter for that hour, typically a weighted average. The result is shown in Figure 2 (right). These values, multiplied by the number of days in the month that that particular value applies (i.e. is non-zero), were added up, coming to a total of 1251kWh/m^2/year, or 3.427kWh/m^2/day. The design DNI values now exceed 800W/m^2 between 10:00 and 14:00 for all months except November, but unlike the average values shown in Figure 2 (left), these design values are not applicable every hour of the year.

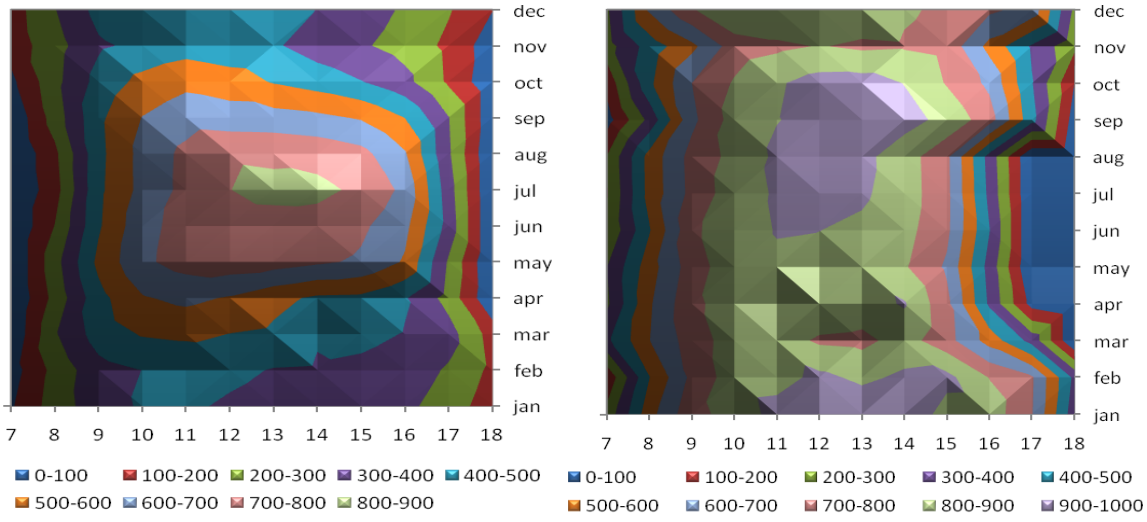

Figure 2: Hourly DNI values for heliostat field design: monthly average (left) and filtered (right)

3. Layout Methodology

The layout was carried out in four steps:

1. initial definition of heliostat positions, using the HFLCAL field layout tool and assuming standard heliostats
2. optimization of canting angles for target-aligned heliostats, using detailed ray tracing analysis (SPRAY)
3. refinement of heliostat positions, using detailed ray tracing analysis (SPRAY)
4. final optimization of canting angles for target-aligned heliostats, using ray tracing analysis (SPRAY)

With HFLCAL it is possible to do heliostat field optimizations for large numbers of heliostats in an acceptable amount of time due to a mathematical simplification: in general, the finite size of the sun, deviations of the mirror curvature and imperfections of the mirror surface are responsible for the final size of the focal spot at a given point in time. All these effects superimposed lead to a variety of directions of the reflected rays which are statistically distributed within some cone around the vector between the heliostat and the target. Additionally, uncertainties of the tracking accuracy of the heliostat enlarge the imprecision of each reflected ray. It is assumed by HFLCAL that the probability of a certain direction of the reflected ray to occur can be well approximated by a circular Gaussian normal distribution [6]. All influences are assumed to be independent and thus the distribution of the reflected beam can be described as superposition of the single circular normal distributions [7].

The ray-tracing tool SPRAY allows details analysis of concentrating solar power systems. This tool was originally based on the MIRVAL computer code [8], but was extensively modified for more flexibility and better performance. The modifications include the simulation of target-aligned heliostats and alternative canting methods. Further model enhancements comprise the automatic variation of relevant simulation parameters for optimization purposes.

3.1 Optimization of Annual Intercepted Energy Yield

The goal of the field layout optimization is to obtain maximum annual energy input to the receiver. This optimization goal was selected since different receiver systems will be tested, thus no specific thermal receiver characteristic was applied in the detailed layout using ray tracing.

The annual energy values are derived from the instantaneous power values by applying specific weighting factors. In other words, each instantaneous power data set from the DNI time series is multiplied by its associated weighting factor to get the monthly energy for this time point. These energy values are then summed up over all months and time points to obtain the annual energy. Using this method, the annual DNI is calculated as 1251 kWh/m²/year for the above described DNI distribution.

4. Initial Layout

The main specifications for the heliostat field layout are summarized in Table 1. The height of the bottom of the heliostat pylons is varied according to the topography of the site (Figure 1, right). The optimization for maximum energy yield was realized by a combination of a genetic and a hill climbing algorithm. A subset of six free parameters which describes the heliostat field and the main geometrical receiver values was used: 1: distance between heliostat rows hypothetically at the tower, 2: a factor which defines the increase of the radial distance of heliostats with the distance to the tower, 3: the radial distance from tower until which heliostats are packed to maximum density and at which staggered positioning starts, 4: the tangential distance of heliostats at which heliostats are positioned again closer to each other and staggering starts newly, 5: the receiver diameter (circular aperture) and 6: the inclination of the receiver.

Value	Description	Remarks
Heliostat parameters		
13.396m²	reflective mirror surface	
4.11m x 3.91m	height and width of mirror surface	
0.87	mirror reflectivity	average mirror reflectivity incl. heliostat outages
3.987mrad	beam error: approximated by Gaussian distributions for sun shape (2.35mrad), tracking error (0.95mrad), slope error (1.3mrad)	$\sigma_{beam\_error} = \sqrt{(2\sigma_{slope})^2 + (2\sigma_{tracking})^2 + \sigma^2_{sun\_shape}} = 3.987 mrad$

Receiver parameters		
19m	tower height	receiver aperture at 16m height
0.95	absorptance receiver	
1.0	emissivity receiver	
90°C	excess temperature of the tubes	
50 W/m²K	convective loss coefficient	
600 / 900 °C	receiver inlet / outlet temperature	
25°C	ambient temperature	
Design parameters		
21st September	design day	
solar noon	design time	
950 W/m²	direct normal insolation (DNI)	at design point
400 kW_{th}	design point power thermal	for solar multiple = 1.8

Table 1: Assumptions for the initial HFLCAL field layout

The results of the HFLCAL optimization are an inclination of the receiver of 27.7°, a receiver aperture diameter of 0.947m and heliostat positions as given in Figure 3. As HFLCAL can currently only simulate standard heliostats with azimuth/elevation drive (not target-aligned), the HFLCAL field layout was first analyzed for the impact of the heliostat configuration. For this purpose three different configurations were analyzed using the ray tracing tool SPRAY.

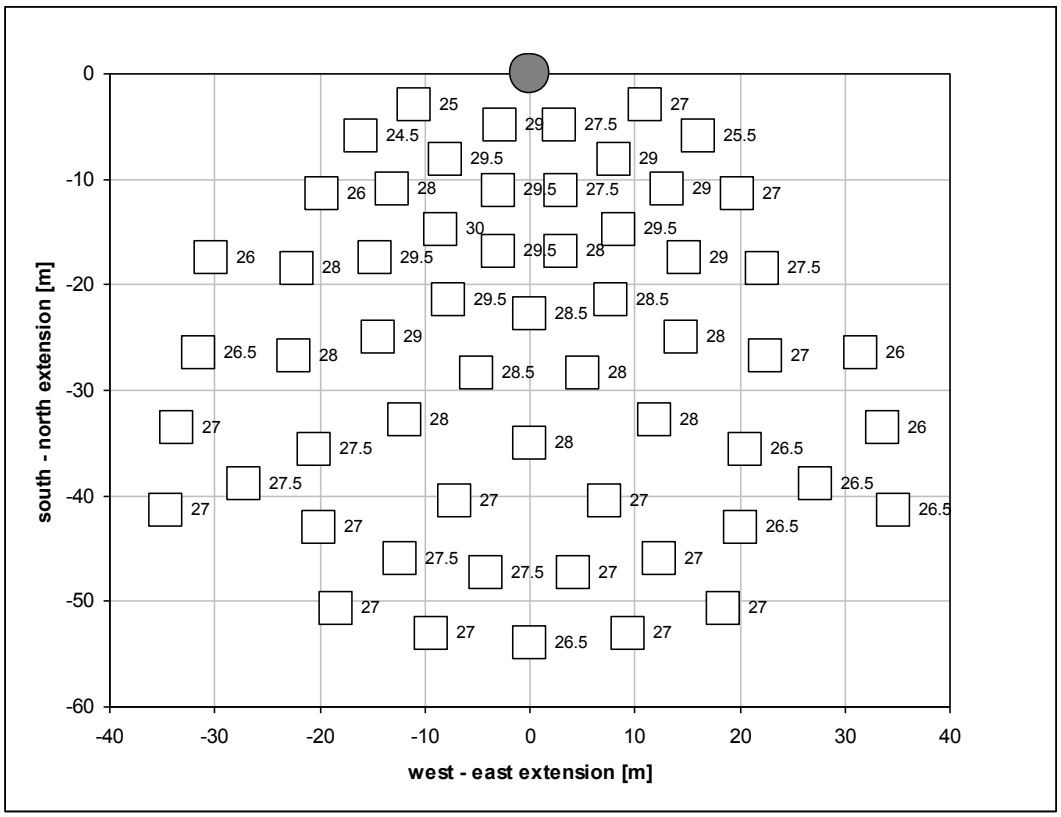

Figure 3: Initial Field Configuration with Canting Angles

The three considered configurations are: 1) standard heliostat with azimuth/elevation drive, on-axis canting, 2) target-aligned heliostat, on-axis canting, and 3) target-aligned heliostat, optimized canting

Canting optimization was performed for each heliostat individually, by changing the incidence angle in the plane perpendicular to the 2nd rotation axis, for the canting situation [4] [5]. For each canting angle the annual intercepted energy was calculated, and the value giving the highest yield was selected as canting angle. The resulting canting angles are given in Figure 3 as number for each heliostat. As the optima are relatively flat, the step width during incidence angle optimization was set to 0.5.

Assuming on-axis canting, there is no significant performance difference between the standard and the target-aligned heliostat configuration. However, when the canting angles for the target-aligned heliostat are optimized, a remarkable improvement of nearly 12% more annual energy output can be achieved.

configuration	**standard heliostat on-axis canting**	**target-aligned hel. on-axis canting**	**target-aligned hel. optimized canting**
intercepted power @ DP [kW]	499.9	498.9 (-0.2%)	526.2 (+5.3%)
intercepted annual energy [MWh]	539.1	541.8 (+0.5%)	586.4 (+8.8%)
receiver thermal output @ DP [kW]	385.0	384.0 (-0.3%)	409.9 (+6.5%)
annual receiver thermal output [MWh]	355.1	357.5 (+0.7%)	396.5 (+11.7%)

Table 2: Comparison of Heliostat Field Performance with Different Heliostat Configurations

5. Field Layout Refinement

Using the initial HFLCAL field layout as start configuration, a non-restricted repositioning of the heliostats is performed in several simulation cycles. In this procedure only target-aligned heliostats are considered. In each cycle the following steps are done:

- evaluation of annual performance of the complete heliostat field in its actual (modified) status
- sorting all heliostats in descending order according to E_{Hi} (annual solar energy contribution intercepted in the aperture)
- repositioning for each single heliostat H_i (in the order of the sorting result above):
  - selection of a sub-group S of 12 heliostats, containing the heliostat selected for repositioning and the closest 11 neighbour heliostats $H_{n,j}$
  - definition of a rectangular 9x8 grid of new positions for H_i around its actual position
  - detection of the *k* neighbour heliostats H_b that can be blocked by H_i in any of the new positions
  - for each of the new position grid points: ray-tracing evaluation of the annual intercepted energy contribution of the heliostat H_i plus the *k* neighbour heliostats H_b; shading and blocking of the complete sub-group S (12 heliostats) is accounted for
  - the position giving the highest annual energy yield is stored as new position for the heliostat H_i and used in sub-sequent simulations

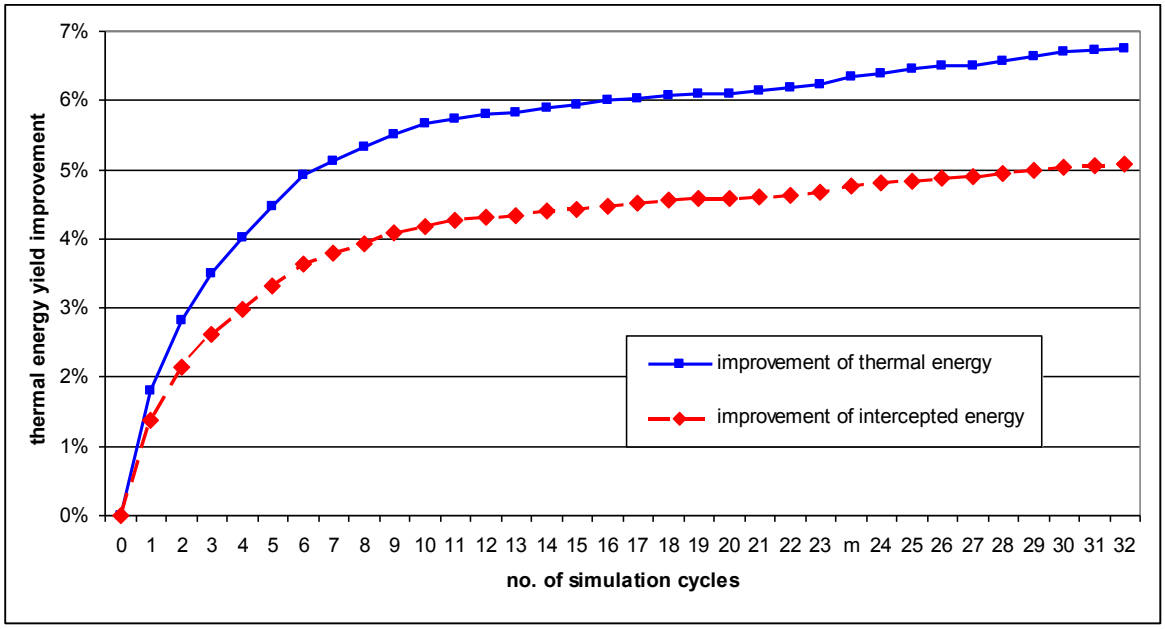

Figure 4: Heliostat Position Refinement Progress

One simulation cycle is completed when all heliostats have been evaluated and (eventually) repositioned. During the repositioning no restrictions were imposed for regular arrangement, except for the requirement of a minimum distance between neighbouring heliostats to avoid contact. The history of the refinement progress is given in Figure 4, showing a significant improvement both in the annual intercepted energy as well as in the absorbed thermal receiver power (taking receiver efficiency into account).

After 23 simulation cycles two heliostats were obviously caught in a local minimum, but at a position which did not look optimal. These two heliostats were repositioned manually (mark “m” in Figure 4). After this manual repositioning, the automatic field refinement was continued without any further manual interaction.

As shown in Figure 4 there is practically no further improvement after 32 simulation cycles, thus the resulting field layout was considered as final. The resulting final heliostat field layout is shown in Figure 5, together with the initial field layout. As can be seen, the unrestricted field optimization led to a final field layout which is less extended in the east-west direction, but slightly shifted away from the tower in south direction.

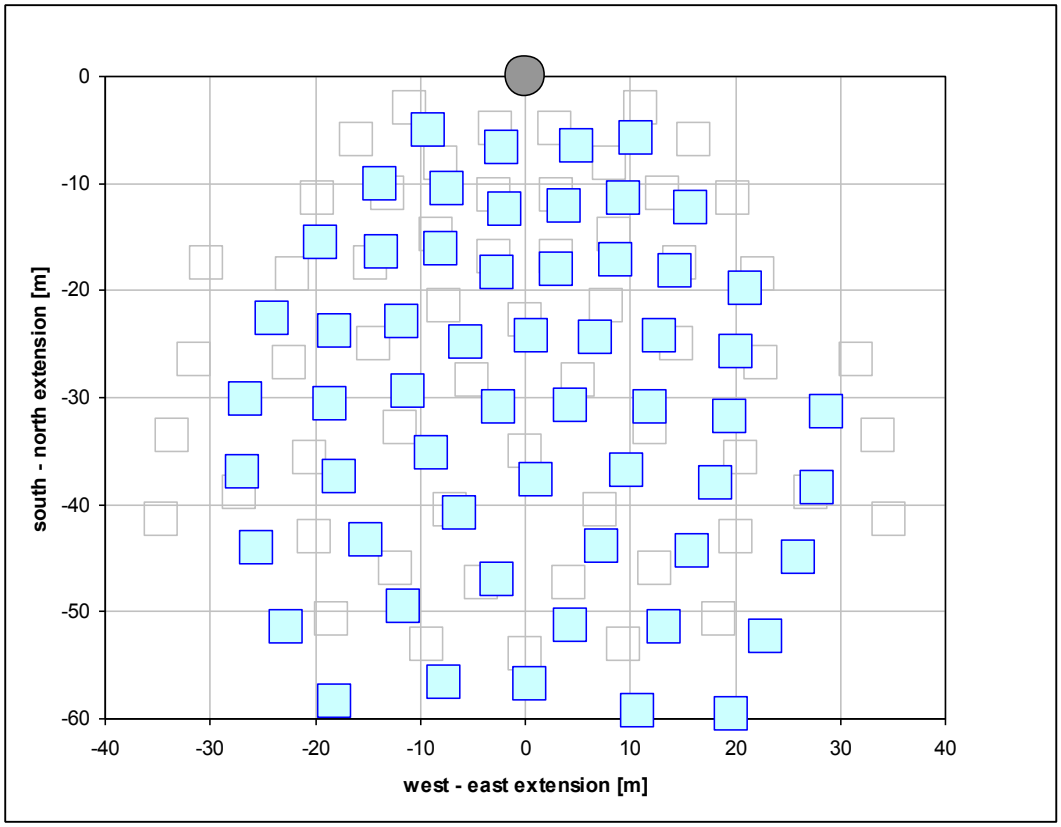

Figure 5: Initial (grey) and Refined (blue) Field Configuration

After freezing the final heliostat positions, the canting optimization was redone to ensure that each heliostat was canted optimally according to its final (modified) position. However, the resulting final canting angles do not differ much from the initial ones. The resulting performance gain is summarized in Table 3. A significant improvement of +5.1% in the intercepted annual energy and of +6.8% in the annual thermal energy was achieved due to the repositioning. The repositioned field is narrower in the east-west direction, but somewhat shifted towards south direction.

Redoing the canting angle optimization for the final layout resulted in a small additional improvement in the annual intercepted and thermal energy (less than 0.1%). This result clearly shows that the constraints imposed by the correlation-based field layout in HFLCAL (with only a few parameters for optimization) are not leading to the optimal field design, but can be significantly improved.

field layout with target-aligned heliostats	initial position (reference)	after position refinement	after final canting optimization
intercepted power @ DP [kW]	526.2	538.3 (+2.3%)	538.0 (+2.2%)
intercepted annual energy [MWh]	586.4	616.1 (+5.1%)	616.4 (+5.1%)
receiver thermal output @ DP [kW]	409.9	421.4 (+2.8%)	421.1 (+2.7%)
annual receiver thermal output [MWh]	396.5	423.3 (+6.8%)	423.5 (+6.8%)

Table 3: Comparison of Heliostat Field Performance before and after position refinement

6. Conclusions

The layout for a solar tower test facility for CSIR, Pretoria, with 400kW$_{th}$ receiver design power was made. The heliostat field layout takes into account both the real (non-flat) topography of the terrain as well as the typical weather conditions at the site, with usually better solar conditions in morning times. As a first step, an initial field layout was done assuming standard heliostats. Then, the performance improvement due to the use of target-aligned heliostats was evaluated, showing nearly 12% gain in annual energy when optimized canting angles are applied to each heliostat.

In a second step the positions of the heliostats were adjusted to further improve the annual energy yield. This was done by slightly shifting the position of a heliostat and evaluating the impact on annual energy yield. No restrictions were made on the heliostat positions, except for a minimum distance between neighbouring heliostats. The heliostats were repositioned one after the other for the whole field. This procedure was repeated many times. At the end of this optimization, the annual thermal energy was about 6.8% higher than the initial layout with target-aligned heliostats, and about 19.3% higher than the initial layout with standard heliostats.

References

[1] Roos T. H., Buck R., Pfahl A. (2009), Design of a Multi-Purpose Target-Aligned Heliostat Field, Proceedings ISES SWC 2009, 11-14 October 2009, Johannesburg

[2] Igel E. A. and Hughes R. L., (1979), “Optical Analysis of Solar Facility Heliostats”, Solar Energy, Volume 22, pp. 283–295.

[3] Chen, Y.T., Kribus, A., Lim, B.H., Lim, C.S., Chong, K.K., Karni, J., Buck, R., Pfahl, A., Bligh, T.P., (2004), “Comparison of two sun tracking methods in the application of heliostat field”, Journal of Solar Energy Engineering 126, pp. 1–7.

[4] Buck, R., Teufel, E., Comparison and Optimization of Heliostat Canting Methods. Journal of Solar Energy Engineering, Vol. 131, 1, 2009, doi:10.1115/1.3027500

[5] Zaibel, R., Dagan, E., Karni, J., and Ries, H., 1995, “An Astigmatic Corrected Target-Aligned Heliostat for High Concentration,” Solar Energy Materials and Solar Cells, 37, pp. 191–202.

[6] Pettit R. B., Vittitoe C. N., Biggs F., Simplified Calculational Procedure for Determining the Amount of Intercepted Sunlight in an Imaging Solar Concentrator. Journal of Solar Energy Engineering, Vol. 105, 1983, pp.101-107

[7] Schwarzbözl, P., Pitz-Paal, R., Schmitz, M., Visual HFLCAL – A Software Tool for Layout and Optimisation of Heliostat Fields. In: Proceedings SolarPACES 2009, 15.-18. September 2009, Berlin

[8] Leary, P.L., Hankins, J.D., A User’s Guide for MIRVAL – A Computer Code For Comparing Designs of Heliostat-Receiver Optics for Central Receiver Solar Power Plants. Sandia Laboratories Report, SAND77-8280, 1979